Crystal shapes, triglyphs and twins in minerals: the case of pyrite

Corinne Arrouvel*

DFQM/CCTS, Universidade Federal de São Carlos, Campus Sorocaba, Sorocaba - SP, Brazil

*e-mail: corinne@ufscar.br

FIGURE SI1

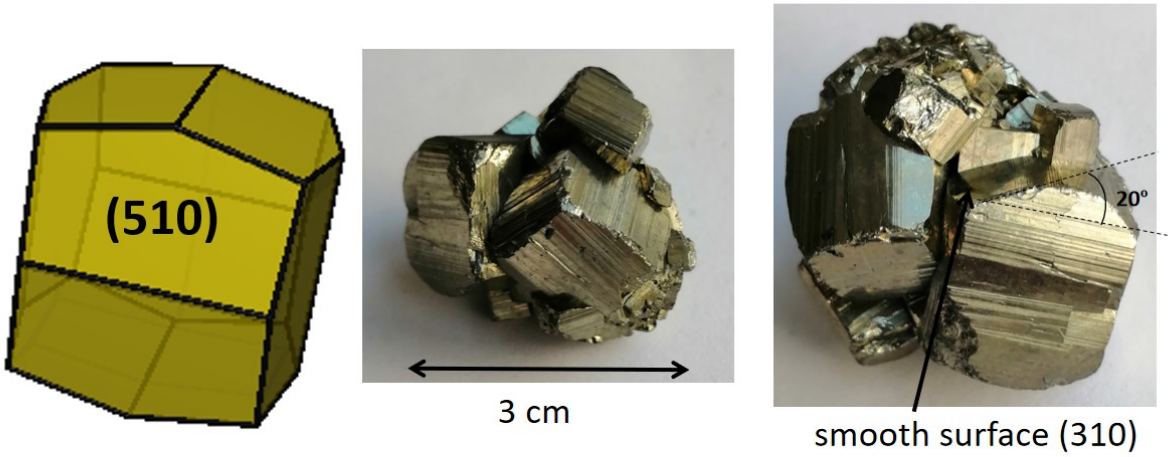

FIGURE S1. Pyrite with intermediate shapes cube-pyritohedron. (**a**) Simulated morphology with {510} surfaces (**b**) pictures with different orientations to highlight *positive* striations and smooth planes onto (hk0) facets , origin Peru.

This sample in Fig. S1 has striations with smoother planes observable at one side, with an (hk0) orientation. An anisotropy is then evidenced, meaning that (hk0) is different from $(h\bar{k}0)$. The angle between planes (hkl) and (h′k′l′) verify using the relation in the cubic system:

$$\cos\theta = \frac{hh'+kk'+ll'}{\sqrt{(h^2+k^2+l^2)(h'^2+k'^2+l'^2)}}$$

The (hk0) plane has roughly an angle of 20º with the (100) plane. The deduced smooth plane is then the (310) plane which is a stable with a low attachment energy (kinetically favorable).

FIGURE SI2

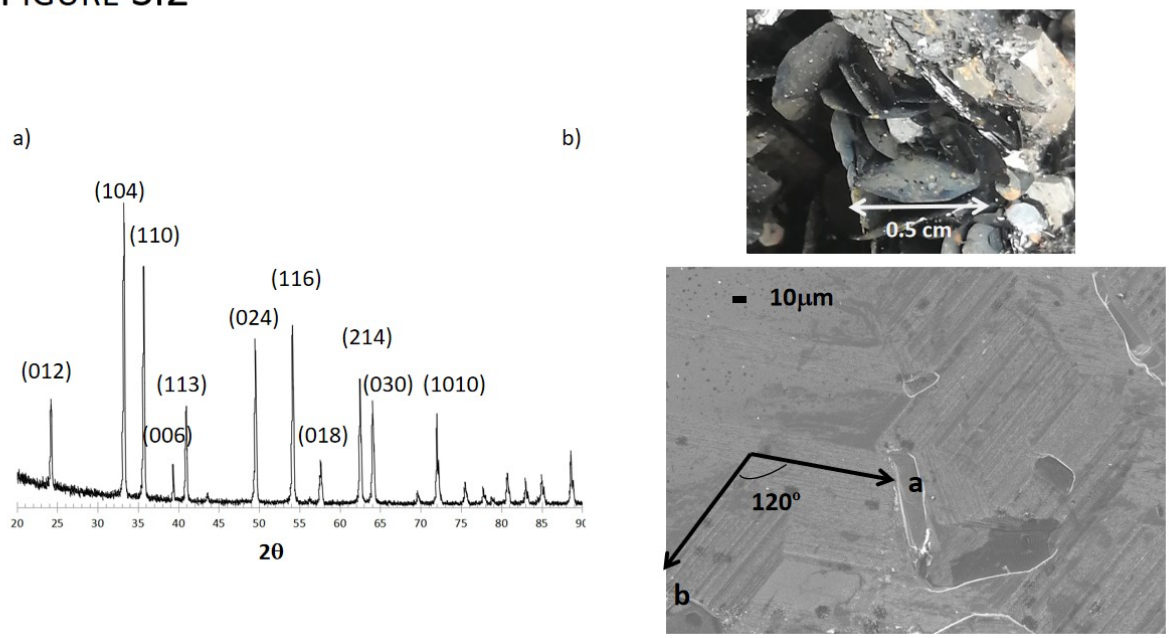

FIGURE S2. Micaceous Iron Oxide hematite, origin Elba, Italy (**a**) XRD (**b**) photograph (by C. Arrouvel) and SEM image.

Micaceous Iron Oxide hematite is growing in contact with negative striated pyritohedral pyrite. The Miller indices follow the structure R-3c (space group number 167).

FIGURE SI3

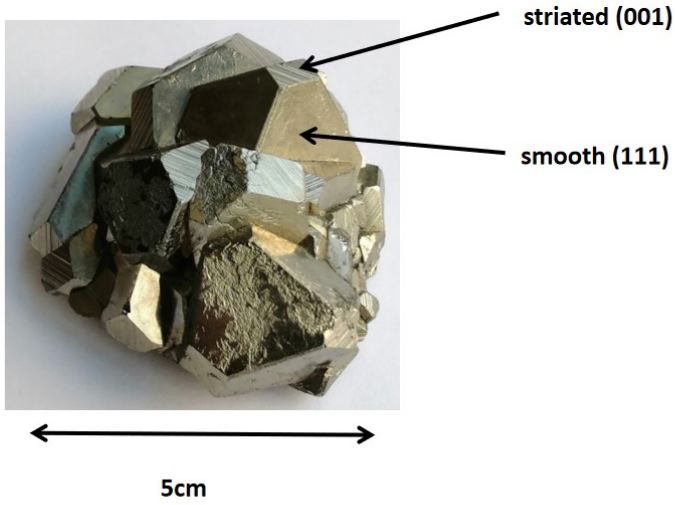

FIGURE S3. Photograph (by C. Arrouvel) of pyrite troncated pyritohedron, origin Peru.

In Fig.S3 are evidenced the striations on {001} facets while {111} facets are smooth.

FIGURE SI4

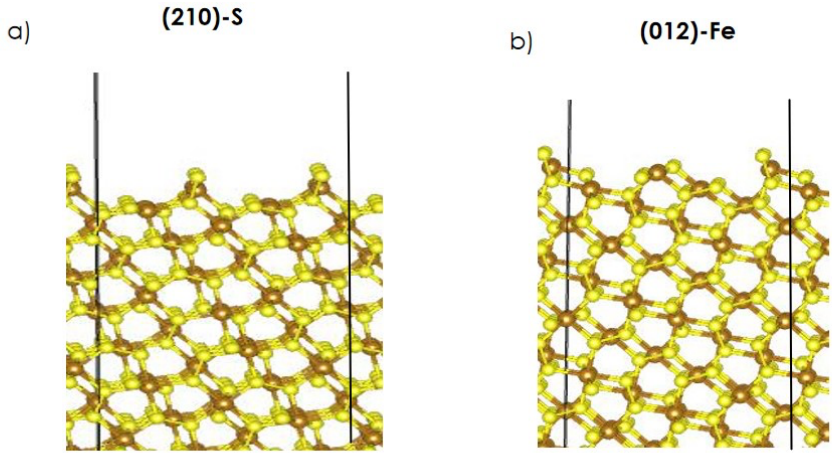

FIGURE S4. Structure of relaxed (**a**) (210) and (**b**) (120) surfaces of pyrite (optimized with force field). (Iron: brown spheres; sulfur: yellow spheres)

FIGURE SI5

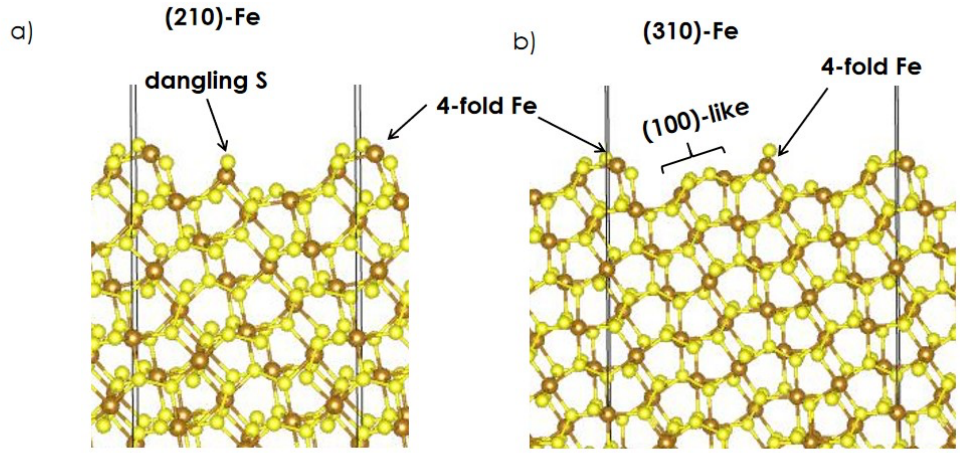

FIGURE S5. Structure of relaxed a) (310)Fe and b) (120) surfaces of pyrite (optimized with force fields). (Iron: brown spheres; sulfur: yellow spheres)

FIGURE SI6

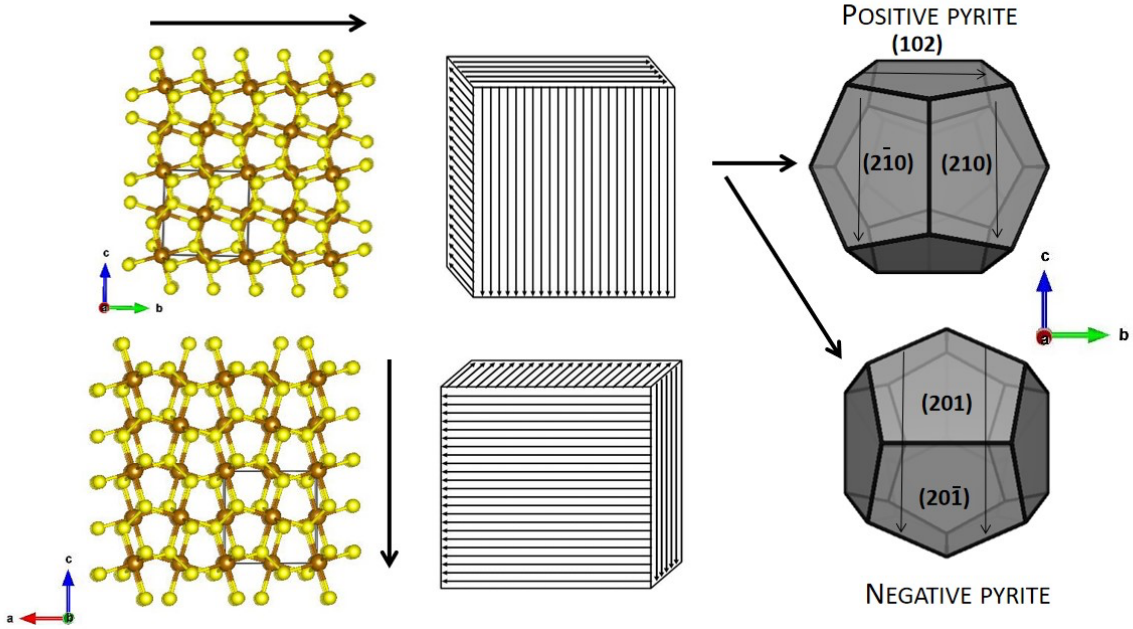

FIGURE S6. Schematic representation of the directions of the striations on the cube in light of sulfur network, in the *positive* {210} pyritohedron and *negative* {120} pyritohedron. (Iron: brown spheres; sulfur: yellow spheres)

FIGURE SI7

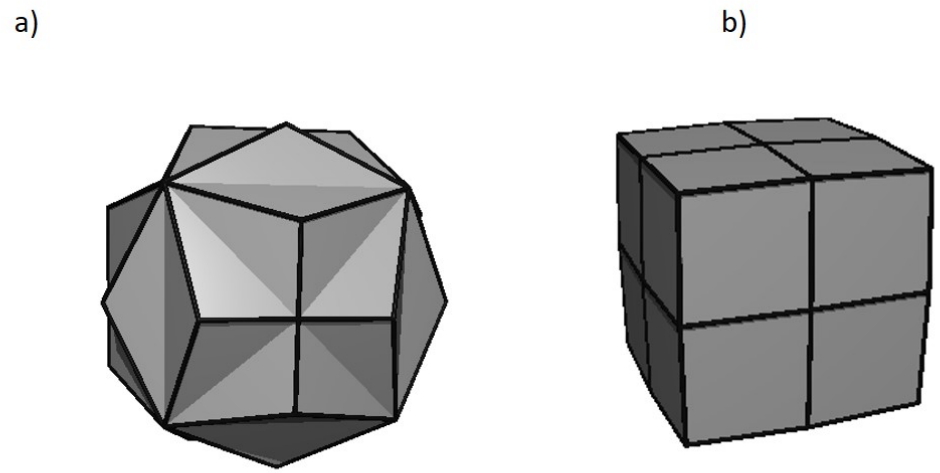

FIGURE S7. $[100]_{90°}$ twinning axis of two penetrating (**a**) pyritohedral crystals; (**b**) anisotropic cubical crystals to illustrate the Fig. 2c from Alonso-Azcárate et al. (2001) (for visualization purpose, the twinned cubes with {40 1 1} facets have been simulated).

FIGURE SI8

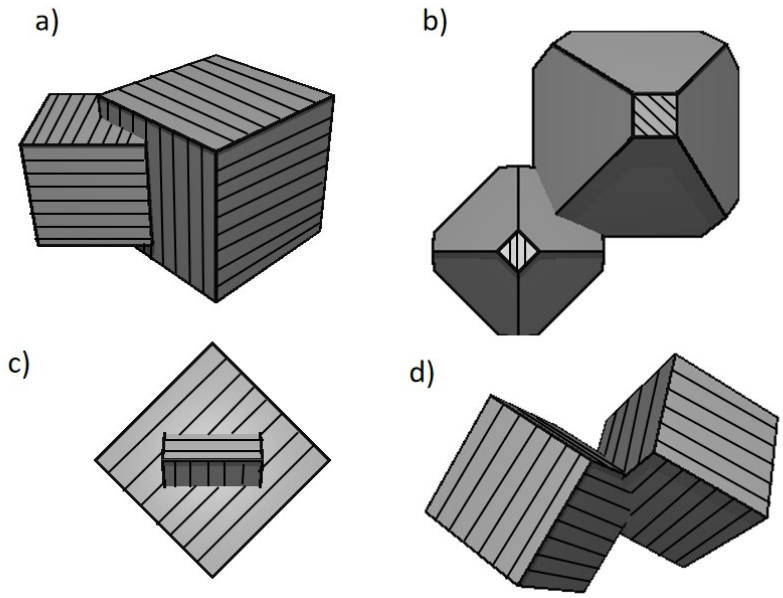

FIGURE S8. (**a**) Cubes with $(100)/(\bar{1}10)$ interface using a $[001]_{45^o}$ rotation, (**b**) octahedra with $(100)/(\bar{1}10)$ interface using a $[001]_{45^o}$ rotation, (**c**) cubes with (001)/(101) interface using $[001]_{45^o}$ and $[100]_{45^o}$ rotations (**d**) cubes with a $[110]_{45^o}$ rotation.

The striations are schematized in Fig. S8 as they are helpful to identify types of twinning.

FIGURE SI9

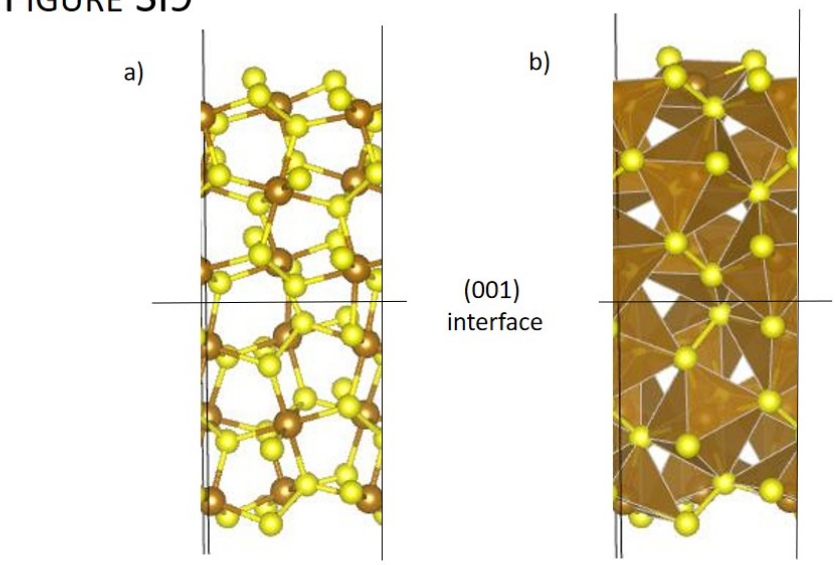

FIGURE S9. Optimized slab of the rotational [001] twinning of (001) slab (DFT method). Ball and stick representation and polyhedral representation. (Iron: brown spheres; sulfur: yellow spheres)

FIGURE SI10

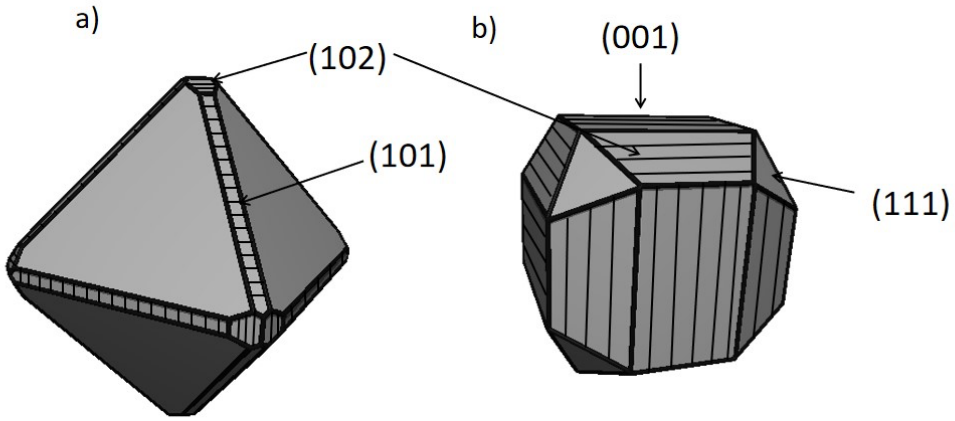

FIGURE S10. Simulations of observed morphologies with surface energy ratios (**a**) (110)/(111) = 1.2 and (210)/(111) = 1.4, (**b**) (210)/(100) = 1.1 and (111)/(100) = 1.2.